frontiers | Frontiers in Environmental Chemistry

TYPE Original Research
PUBLISHED 25 April 2025
DOI 10.3389/fenvc.2025.1568188

OPEN ACCESS

EDITED BY
Erik Björn,
Umeå University, Sweden

REVIEWED BY
Juan Carlos Nóvoa-Muñoz,
University of Vigo, Spain
Hanbing Li,
Nanjing University, China

*CORRESPONDENCE
Peter Weiss-Penzias,
✉ pweiss@ucsc.edu

RECEIVED 29 January 2025
ACCEPTED 31 March 2025
PUBLISHED 25 April 2025

CITATION
Weiss-Penzias P, Straw B, Rothman M, Zheng B, Seelos M, Rivas Meraz E and O'Day PA (2025) Atmospheric mercury uptake to foliage using *in situ* and transplanted lichens at the New Almaden Mining District, California, United States. *Front. Environ. Chem.* 6:1568188. doi: 10.3389/fenvc.2025.1568188

Atmospheric mercury uptake to foliage using *in situ* and transplanted lichens at the New Almaden Mining District, California, United States

Peter Weiss-Penzias[1]*, Brittney Straw[1], Michelle Rothman[1], Belle Zheng[1], Mark Seelos[2], Edwin Rivas Meraz[3] and Peggy A. O'Day[4]

[1]Department of Microbiology and Environmental Toxicology, University of California, Santa Cruz, Santa Cruz, CA, United States, [2]Santa Clara Valley Water District, San Jose, CA, United States, [3]Environmental Systems Graduate Group, University of California, Merced, CA, United States, [4]Department of Life and Environmental Sciences and Environmental Systems Graduate Group, University of California, Merced, CA, United States

Contaminated soils at former mercury (Hg) mines release Hg into the atmosphere that can be absorbed by the surrounding foliage and potentially contribute to inputs of Hg to downstream reservoirs and the food chain. Information on Hg re-emissions and atmospheric transport at the New Almaden Mining District (NAMD) in California's Coast Range is lacking, despite the wealth of previous research at the site. This study addressed knowledge gaps regarding the locations of the highest Hg re-emissions using *in-situ* and transplanted lichens. High total Hg (THg) concentrations in lichen (up to 20 μg g^{-1}) were found where ore-processing occurred pre-1900 and where the largest mines were. Mean background concentration of THg in lichen (156.3 ± 48.2 ng g^{-1}) was observed >7.8 km away from the most contaminated site. Lichen THg was significantly higher than the background by 93–171 ng g^{-1} at locations along the shorelines of three small reservoirs in the NAMD. By transplanting lichens from background areas to three sites in the NAMD, statistically significant first-order rate constants of Hg uptake (0.0011–0.0036 $days^{-1}$) were found. The trend in uptake rate constants matched the trend in THg concentrations in non-transplanted lichen and atmospheric concentrations monitored by Hg passive samplers. There was no trend in the control transplants nor in release rates. Speciation analysis of lichen samples collected from sites of highest contamination using Hg High Energy Resolution Fluorescence Detection (HERFD) XANES showed the dominance of α-HgS (cinnabar) in spectra, likely present as nanoparticles, in addition to variable Hg coordination by dithiol, sulfide, and chloride ligands at the micrometer scale. These results indicate that the majority of Hg in lichen is associated with non-volatile phases and/or organic species and suggest that a relatively small fraction of Hg exchanges with the atmosphere, in agreement with relatively low uptake rates. Overall, study results

show that THg concentrations in lichen surveys have merit across gradients of contamination and indicate that Hg deposited to lichens is likely sequestered for many years before entering the soil as litterfall.

KEYWORDS

mercury, lichen, bioindicator, mercury mine, watershed, HERFD XANES (X-ray absorption near edge structure), transplantation

1 Introduction

The global mercury biogeochemical cycle is a complex cascade of fate, transport and bio-uptake and due to its ability to persist in the environment and bioaccumulate in food webs, it poses a risk to ecosystems and human health (Selin, 2009; Sonke et al., 2023). Mercury is a naturally occurring element within Earth's biogeochemical system and can be released into the atmosphere through natural and anthropogenic sources (Pirrone et al., 2010; Jiskra et al., 2018). Atmospheric Hg, which is primarily Hg^0, can be taken up by plants and lichens in the terrestrial ecosystem much like CO_2 (Jiskra et al., 2018) or as Hg^{II} species during wet deposition (Sonke et al., 2022). Litterfall releases Hg to aquatic and soil systems where anaerobic bacteria reside and are responsible for methylating Hg (Jiskra et al., 2018; Huang et al., 2023), whereas several biotic and abiotic processes have been identified for methylmercury demethylation (Barkay and Gu, 2022). Contaminated sites where Hg ore and other minerals were mined contribute a significant quantity of Hg to the atmosphere through geogenic emissions and anthropogenic re-emissions (Kocman et al., 2013; Eckley et al., 2020; Eckley et al., 2023). In particular, the historical mine waste dumps of inefficiently roasted cinnabar (α-HgS(s)) are an important source of environmental Hg contamination through volatilization of Hg and wind entrainment of Hg bound to dust particles (Gustin et al., 2003). Total mercury concentration in soil, soil temperature, light energy, rainfall, and vegetation can influence the amount of Hg emitted from soil (Fantozzi et al., 2013). This has been demonstrated and studied in historic Hg mining areas such as the Almadén mining district (Spain) and the Idrija mining districts (Slovenia) (Jiménez-Moreno et al., 2016; Božič et al., 2022). Foliage many kilometers distant from the center of Hg contamination is often contaminated from Hg dry and wet deposition. Downstream aquatic systems are then potentially impacted by Hg deposition to the foliage across whole-watershed scales through litterfall and runoff (Eckley et al., 2023).

While the negative ecosystem effects of Hg mines have been relatively well-characterized for the largest sites in Europe, little attention has been paid to understanding Hg deposition around important mines in the California Coast Range, in particular the New Almaden Mining District (NAMD). The NAMD is located south of San Jose, California, and was once the largest cinnabar mine in North America from 1845–1971 (Cargill et al., 1980). Legacy mine waste continues to be a constant source of Hg contamination in the Guadalupe River Watershed, which includes the Guadalupe, Calero, and Almaden Reservoirs (McKee et al., 2017). Each reservoir contains fish that exceed the regulatory threshold for Hg concentrations despite active remediation efforts (Seelos et al., 2021). These reservoirs are connected to the San Francisco Bay via the Guadalupe River, which is subject to a State of California Water Board Total Maximum Daily Load regulatory threshold for Hg (Thomas et al., 2002; Conaway et al., 2004; Gehrke et al., 2011). Despite the high levels of contamination in this region from legacy mining activities, there are no reported measurements of Hg emissions to the atmosphere, limiting our understanding of the spread of Hg aerially. Atmospheric Hg monitoring is needed to accurately determine the transport and fate of Hg emissions around these former mining areas.

In recent decades, lichens have been one of the most used bioindicators to measure air pollution, particularly heavy metals such as Hg (Abas, 2021). Lichens are a symbiosis composed of a fungus (mycobionts) and green algae or cyanobacteria (photobionts), together forming a foliar structure called a thallus. The fungus provides the algae with protective sheltering structures, while the algae or bacteria supply photosynthetically fixed carbon as an energy source (Garty, 2001; Conti and Cecchetti, 2001; Bargagli, 2016). Lichens are ubiquitous across the globe, as they are perennial organisms and can grow in nearly all habitats. Lichens primarily receive nutrients from the atmosphere as they lack a vascular and root system, thus making them ideal as an atmospheric bioindicator. Furthermore, lichens do not possess a waxy cuticle, allowing them to accumulate atmospheric nutrients and metals across the thallus surface (Weissman et al., 2005). Although different lichen species are well known for their ability to act as biomonitors of Hg, radionuclides, and metals, there remain knowledge gaps surrounding the physiological processes associated with metal uptake, biochemical transformations, and accumulation (Bargagli, 2016; Anderson et al., 2022; Thakur et al., 2024). Lichens can acquire Hg by gas exchange, wet deposition, and entrapment of particles. Studies of Hg isotope fractionation have lent insight into Hg uptake by lichens and indicate that both gas exchange of Hg^0 and wet deposition of Hg^{II} species are important pathways despite the dominance of Hg^0 in the atmosphere (Božič et al., 2022; Sonke et al., 2023). Once in contact with the organism, the molecular fate of Hg is not known in detail, but studies suggest that Hg^0 may be re-released or evaporated, and a fraction as Hg^{II} is sequestered by phytochelators as a defense mechanism against toxicity (Bargagli, 2016; Thakur et al., 2024). Given the strong affinity of Hg for reduced sulfur ligands such as thiol and sulfide, phytochelatins containing cysteine or glutathione are thought to be involved in either intracellular or extracellular sequestration (Seregin and Kozhevnikova, 2023; Thakur et al., 2024). Lichens can take up other heavy metals including Cu, Fe, and Pb, which can degrade chlorophyll and produce reactive oxygen species in the cells, thereby affecting the health of the lichen (Thakur et al., 2024). However, the effect of other metals on the effectiveness of Hg uptake has not been quantified.

Two main types of research have been conducted using total Hg concentrations in lichen bioindicators: the identification of

emissions hotspots due to re-emissions from contaminated soils especially around mining sites (Berdonces et al., 2017; Demková et al., 2023; Gačnik et al., 2024), and lichen transplantations in which clean lichen are exposed to a contaminated environment (or vice versa) to determine the rate of uptake (or release) (Loppi et al., 1998; Ljubič Mlakar et al., 2011; Berdonces et al., 2017; Monaci et al., 2022; Bubach et al., 2024). Some recent studies also incorporated passive and active atmospheric Hg sampling as a comparison with the Hg levels found in lichens (Monaci et al., 2022; Gačnik et al., 2024). It has been noted that using total Hg (THg) concentrations in lichen to infer Hg atmospheric deposition can present difficulties due to the influence of climatic and environmental conditions that affect metabolic growth rate and the deposition and bioavailability of Hg (Bargagli, 2016; Zvěřina et al., 2018; Božič and Horvat, 2024). The use of stable isotopes of Hg in addition to total concentration provides more interpretive power (Sonke et al., 2022; Božič and Horvat, 2024), but Hg isotope measurements can be challenging and expensive. Lichen biomonitoring of THg concentrations, which are easily measured at relatively low cost, can serve as a creative technique for studying airborne Hg and other elements if the influences of climatic and microclimatic effects are considered when interpreting the data (Zvěřina et al., 2018). Despite the scientific value, using lichen bioindicators has scarcely been practiced in North America (Nash and Sommerfeld, 1981; Rope and Pearson, 1990; Sweat, 2010; Wiederhold et al., 2013; Root et al., 2013; Will-Wolf et al., 2017; Weiss-Penzias et al., 2019).

Element-specific spectroscopic methods such as synchrotron X-ray absorption spectroscopy (XAS), including X-ray absorption near-edge structure (XANES) and extended X-ray absorption fine structure (EXAFS) spectroscopies, have been used to identify Hg molecular speciation in plant leaves (Carrasco-Gil et al., 2013; Manceau et al., 2018) and pine bark (Chiarantini et al., 2017; Bardelli et al., 2022) near mining sites, but not in lichens to our knowledge. Prior studies employing conventional XAS have been limited to relatively high THg concentrations (>~30 μg g^{-1}) in order to obtain sufficient spectral signal to noise. High Energy Resolution Fluorescence Detection (HERFD) XANES is a new variation of the conventional XAS method that adds a set of spherically bent crystal analyzer spectrometers aligned on a Rowland circle to focus fluorescence from the sample to the detector (Sokaras et al., 2013). Scanning incident energy over a core-level absorption edge (typically Hg L_3) while simultaneously focusing the emission maximum of a specific fluorescence line (e.g., $L\alpha_1$ emission for Hg) selects a narrow energy range from the total fluorescence signal, known as resonant inelastic X-ray scattering (RIXS) (Glatzel et al., 2013). Significant sharpening of XANES absorption features results from a combination of factors: reduction in the intermediate and final state core hole lifetime broadenings; lower instrumental broadening, which includes monochromator resolution at the energy of the incoming radiation and energy resolution of the crystal spectrometers; and reduction of background noise by using only a narrow energy range for measurement (Glatzel et al., 2013; Sokaras et al., 2013; Nehzati et al., 2022). As a result, the HERFD XANES method improves identification of element local bonding environments associated with specific phases or complexes, and has higher sensitivity, enabling measurements down to environmentally relevant concentrations of around 1 μg Hg g^{-1} or less.

In this study we identified and quantified areas of high Hg atmospheric emissions in the NAMD by measuring the total Hg (THg) content of lichens across a spatial gradient, targeting areas of known historical activity, and across time using lichen transplant experiments, to better understand the impacts of these emissions on local reservoirs and the watershed. This study addressed how distance from the center of mining activities relates to Hg contamination near a reservoir, emission rates of Hg from soils at locations with different levels of Hg contamination, and Hg washability from lichen surfaces as an indicator of mobility. We discuss uncertainties associated with lichens as a bioindicator and the use of single or multiple lichen species for biomonitoring. In addition, selected samples from an area of high Hg contamination were investigated with Hg $L\alpha_1$ HERFD XANES spectroscopy to reveal molecular-level Hg speciation in lichens and its potential for reactivity and volatility.

2 Materials and methods

2.1 Sampling locations

Lichens were sampled across a range of locations in the southern San Francisco Bay area (Figure 1) characterized by oak woodlands. Background locations were defined as >20 km outside the NAMD, although various other Hg sources in the region like cement plants, small and long-abandoned Hg mines, and other industries may have impacted the Hg levels in these locations. However, the areas in the NAMD where mining and ore processing activities occurred are grossly contaminated compared to all sites outside the NAMD and these areas were targeted for more intensive sampling. The largest and oldest of these sites is the Hacienda Furnace Yard (HAC) where ore was roasted, and Deep Gulch where waste was dumped starting in the 1850s. Of all areas in the NAMD, HAC was where approximately 96.5% of the Hg production occurred (Cargill et al., 1980). The soil contains calcine fragments and layers that are contaminated with Hg^0 (Bailey and Everhart, 1964). Another contaminated site is Mine Hill, where from 1940–1971, ore from a combination of open pit and underground mines was roasted in a rotary kiln. Other sites sampled included the sites of the former Senador Mine, the Enriquita Mine, and the San Mateo Mine, located in the northern part of the NAMD. Lichens were sampled with the aid of a boat, along the shorelines of three reservoirs: Calero (CR), Almaden (AR), and Guadalupe (GR). AR and GR are within the NAMD and CR is just outside the NAMD, although it is connected to the AR via a canal. A site at the Lexington reservoir (LR) was selected as the background site for the transplantation experiments due to THg concentrations in lichens that were representative of the other background sites sampled, a variety of lichen species present, and easy access in this Santa Clara County Park.

2.2 Lichen sampling and sample preparation

Lichens were collected from locations across the NAMD and background areas mainly from these tree species where heavy lichen growth on easy to reach branches occurred: coast live oak *(Quercus agrifolia),* Shreve oak *(Quercus parvula* var. *shrevei),* and blue oak

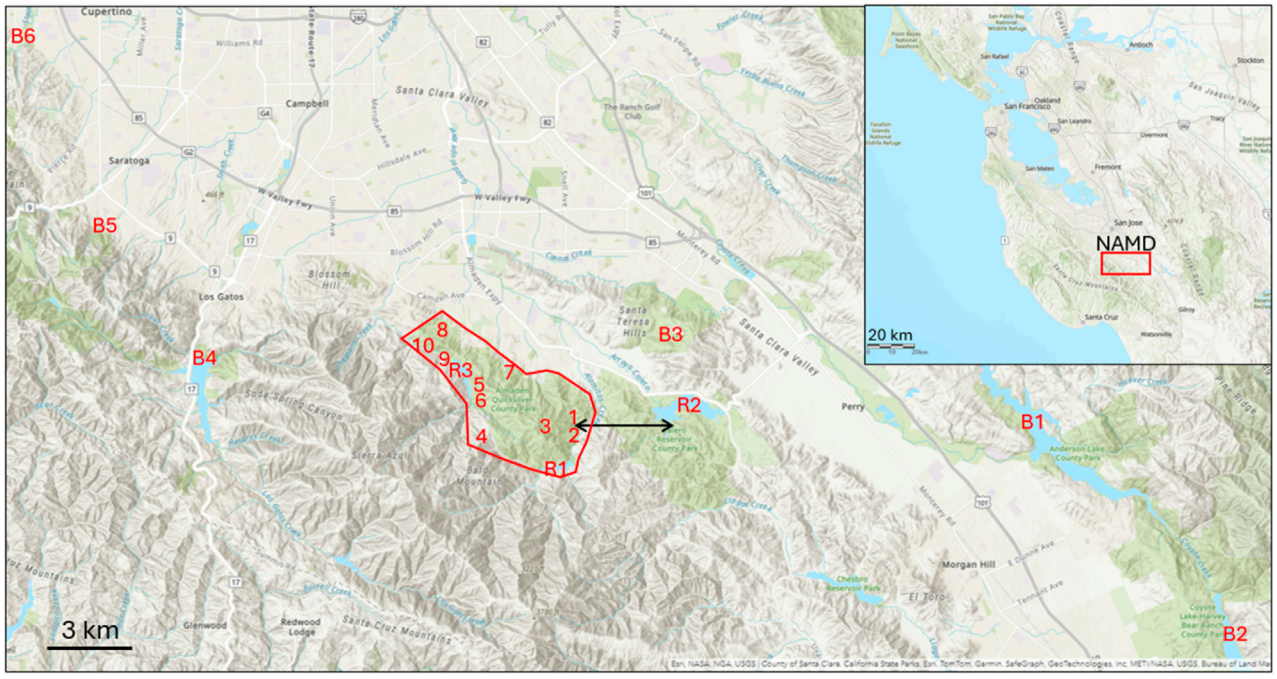

FIGURE 1
Map showing the New Almaden Mining District (red polygon) in the California Coast Range and relative to other locations where lichen were sampled. Site codes refer to the data shown in Table 1 and the black arrow shows the 3.2 km transect line from Hacienda Furnace Yard (1) to Calero Reservoir (R2).

(Quercus douglasii). Lichens were collected in large clumps until about 250 mL of loosely packed volume was obtained. A clean gloved hand or a methanol-cleaned 6 m telescoping fruit picker was used to sample the lichen after which it was stored in two polyethylene zip-closure storage bags in a cooler. Coordinates of each sampling location were determined using Google Maps. The lichen samples were brought back to the lab at University of California Santa Cruz, where the lichen species were identified and the relative proportions in each sample were noted using a field guide, then stored until further processing in the lab freezer at −20°C. Six species were used in this study: *Evernia prunastri* (EP), *Ramalina farinacea* (RF), *Ramalina menziesii* (RM), *Ramalina leptocarpha* (RL), *Flavopunctelia sp*. (FL), and *Usnea* sp. (US) (Supplementary Figure S1). All foreign materials, such as tree bark, leaves, insects, and other plants, were removed from the lichen samples. A portion of the samples was washed with deionized water or a 1% EDTA solution, as described in Windham-Myers et al. (2014).

Lichen samples were homogenized either as individual species in the case of the samples from background locations and from the transplantation experiments, or as a mixed-species sample when collected at different locations in the NAMD (Barre et al., 2020). Species composition in terms of approximate % by volume for each of the six species targeted was noted at this time. Variation in THg concentrations between species is discussed below. Homogenization was done by taking 50–250 mL of loosely packed lichen (depending on how much had been collected) and crushing with liquid nitrogen and a mortar and pestle that was washed with soap and hot water, then acid and deionized water rinsed between samples. The pulverized lichen was transferred to a 20 mL or 40 mL glass vial, or a 50 mL polypropylene centrifuge tube and then lyophilized for 24 h. Once dried, the samples were stored in the dark at ambient indoor temperature.

2.3 Lichen transplantation procedure

For the Hg uptake experiments, lichen was sampled from the background location (LR) in January 2023 (Transplant #1) and in August 2023 (Transplant #2) and transplanted at eight spots in three general locations in the NAMD (Figure 4). Transplants 1–3 were at Mine Hill (MH), transplants 4 and 5 were at Almaden Reservoir (AR) and transplants 7–9 were at the Hacienda Furnace Yard (HAC). Transplant 6 was at LR as a background control site. Transplant controls were conducted by transplanting the lichen found at a given site at that site. Before transplanting, all lichen was rinsed using spring water, laid out on lab wipes on a portable table in the field and patted dry with lab wipes (Adamo et al., 2008). Lichens were separated by species and placed loosely into acid-cleaned 2-L nylon mesh bags (Capozzi et al., 2023). The bags were hung under clear plastic bird feeder rain shields and suspended from oak tree branches at a height of 2 m (Supplementary Figure S2). They were situated out of sight off the main trails at the Almaden Quicksilver County Park. Each rain shield contained at least three hanging bags. Three lichen species (EP, RL, and US) were used for the transplants, which were the abundant species found at all the locations. Data from three NAMD locations plus the background were obtained in transplantation #1, and during transplantation #2, data from one test location (the most contaminated area) plus the background location were obtained. Lichens were sampled every 30 days for nine

sampling events during transplantation #1 and every 60 days for six sampling events in transplantation #2. When sampling from the mesh bags, a volume of approximately 50 mL of loosely packed lichen was subsampled from each bag at each visit.

2.4 Deployment of passive samplers

Tekran® MerPAS passive samplers were deployed in duplicate on 8 cm angle brackets attached to trees at 2 m height, at multiple locations within 30 m of each transplantation site (Supplementary Figure S2 sites (N = 12), the second deployment was February 17 – April 21 (63 days) at HAC (N = 4), the third deployment was March 20 – 19 May 2023 (60 days) at HAC (N = 2), and the fourth deployment was August 14 – 18 Oct 2023 (65 days) at HAC (N = 4). Three field blanks were also included, in which the MerPAS samplers were transported to the field but not opened or deployed.

2.5 Mercury analysis methods

Lichens were analyzed for total mercury concentrations (THg) at UC Santa Cruz using direct mercury analyzer atomic absorption spectroscopy (DMA-80) (Milestone Corp.) following EPA method 7,473. Approximately 0.01–0.05 g of the dried lichen samples were scooped into blanked quartz or nickel sample boats and placed into the DMA-80. Lichen samples were analyzed in duplicate and were quantified against liquid Hg standards (NIST-3133). Certified reference materials (CRM) dogfish liver (DOLT-3) and peach leaves (NIST) were run every 20 samples for QA/QC. The mean recovery of THg in fish liver (DOLT-3 CRM) was 102% ± 2.9% (N = 24) and 92% ± 39% (N = 18) for peach leaves (NIST 1547 CRM). The average %RPD between duplicate lichen sample runs was 16%.

The activated carbon in the MerPAS passive samplers was analyzed at the USGS Mercury Research Laboratory in Madison, WI using a manual combustion furnace, trapping into a chemical oxidant trap, and subsequent analysis using cold vapor atomic fluorescence spectrometry following methods outlined elsewhere (Sun et al., 2013). All activated carbon in each MerPAS was combusted in a single boat for the samples, except for a check sample which was divided into three sub-samples and analyzed individually. To ensure sample recovery, NIST 2691 (coal fly ash) was measured every 5 samples and recoveries ranged from 99%–105%.

2.6 HERFD XANES data collection and analysis

High Energy Resolution Fluorescence Detection (HERFD) XANES spectra at the Hg-L_3 absorption edge and measuring the Hg $L\alpha_1$ emission line were collected at Stanford Synchrotron Radiation Lightsource (SSRL) on beamline 15–2. Incident X-ray energy (I_0) was tuned using a Si (311) double crystal monochromator and Hg $L\alpha_1$ emission was focused using a 7-element array of spherically bent Si (555) crystal analyzers with Johann-type geometry (Sokaras et al., 2013). Samples were maintained in a helium flow cryostat (Oxford instruments, Abingdon, United Kingdom) at a temperature of 10–12 K and positioned at a 45° angle to I_0, which was measured with a gas-filled ion chamber. Fluorescence as a function of I_0 was measured using a single-element silicon-drift Vortex detector (Hitachi High-Technologies Science America Inc., Northridge, CA, USA) with 1.2 mm slits. Emission energy was scanned for each sample and the maximum emission was set at 9,988.9 ± 0.1 eV. Beam size on the sample was 115 × 610 μm for all samples except for AQ30JM4 where beam size was 150 × 700 μm. A reference spectra library consisting of ~40 pure Hg compounds, natural Hg mineral samples, and Hg complexes in aqueous solution was assembled over multiple runs. Reproducibility among runs was carefully verified using identical conditions, primary and secondary calibration standards, and replicate collection of reference compounds (see Supplementary Material).

For dried, powdered lichen samples, a survey scan vertically across the sample was done to locate regions of high and low Hg concentration (determined by fluorescence counts). A region with roughly average Hg was selected for XANES spectra collection except for sample HAC4 for which two sets of spectra were collected. HAC4-1 was a Hg hot spot with high counts where two scans were collected at the same position, and HAC4-2 was an area of lower average Hg counts for which the vertical (z) position of the beam was moved by 230 μm between each scan. Scans with similar features were averaged (14 scans) to improve signal to noise. Similarly for sample AQ22BM1, four similar scans were averaged from four different nearby z-positions. Sample AQ30JM4 had low average counts, and 22 scans were averaged from a single position with no evidence of beam damage (determined by examining spectral features in sequential scans). Fluorescence counts were divided by the incoming beam energy, and XANES spectra were averaged and normalized to the post-edge background. Lichen sample spectra were evaluated using least-squares linear combination (LC) fitting with reference spectra to determine the primary components and bonding environment of Hg comprising the spectrum (see Supplementary Material for analysis details and Supplementary Table S2 for reference spectra).

2.7 Data analysis for Hg uptake rates

Total Hg concentrations measured during the transplantation experiments were used to calculate the first order kinetic factor q_L/q_L^0 which is the species-specific lichen THg concentration at any time divided by the lichen THg concentration at time 0 (Berdonces et al., 2017). A mean value of the time 0 THg concentrations for each species from each location was used for the calculation of q_L^0 (Supplementary Figure S3). Uptake and release rate constants were determined by finding the slope in the units of d^{-1} from a linear fit of q_L/q_L^0 vs. day of lichen transplant. This factor allowed for pooling the time point THg concentrations for different lichen species to increase the overall number of samples used to determine uptake or release rate constants. The slopes of the linear fits were found to be significantly different from zero if an ANOVA test produced a $p < 0.05$. Sample populations were tested for normality using a Shapiro-Wilk test. A Tukey's HSD test was used to determine if the means of sample populations were significantly different from each other with a test criterion of p <

TABLE 1 THg concentrations in mixed-species lichens collected between 2018 and 2022 aggregated by site name.

Site code	Site name	N (# of lichen samples)	Mean THg (ng g^{-1})	Stdev THg (ng g^{-1})	Median THg (ng g^{-1})	Max THg (ng g^{-1})	Min THg (ng g^{-1})
1	Deep Gulch	19	6,174	5,404	3,727	20,084	896.5
2	Hacienda Furnace Yard	32	2,029	3,360	963	14,881	276.1
3	Mine Hill	57	1,742	2035	1,081	10,541	241.7
4	Hick's Road	7	227.1	51.9	243.6	294.9	157.6
5	Enriquita mine	8	431.1	159.9	459.8	607.9	162.2
6	Providence Mine	5	246.8	46.5	240.9	319.0	202.9
7	Mockingbird Hill	4	299.7	97.9	302.9	412.9	180.0
8	Senador Mine	31	486.8	515.8	320.1	2,612.9	97.1
9	San Mateo Mine	8	260.8	111.8	212.6	455.5	148.0
10	Hick's Flat	9	216.8	75.3	186.6	350.0	132.2
B1	Anderson Lake	1	177.2	—	177.2	177.2	177.2
B2	Coyote Lake	21	182.1	42.9	172.8	278.4	133.4
B3	Santa Teresa	3	188.9	73.4	219.5	241.9	105.2
B4	Lexington Reservoir	24	152.0	49.3	162.1	253.1	53.0
B5	Villa Montalvo	13	133.9	32.6	148.2	173.5	77.2
B6	Stevens Creek	11	169.0	50.2	144.6	257.6	112.7
R1	Almaden Reservoir	8	322.8	123.1	311.4	571.1	194.3
R2	Calero Reservoir	25	246.5	66.2	235.2	423.9	147.4
R3	Guadalupe Reservoir	17	275.7	90.8	251.2	522.8	161.7

The site codes are mapped in Figure 1. The numbers refer to sites in the NAMD, B refers to background locations and R refers to reservoir locations.

0.05. All statistical analysis was performed using OriginPro 2024b (OriginLab Corp).

Uptake rates in units of ng g^{-1} d^{-1} were determined for the passive samplers by dividing the field blank corrected THg concentration in the activated carbon sampled at the end of the deployment, by the number of deployment days, which varied between 60–65 days. Uptake rates for the species-specific lichen transplants that were alongside the passive samplers were calculated by subtracting the time zero THg concentration from the end-time THg concentration and then dividing by the number of deployment days. Hotspot mapping was done using Empirical Bayesian Kriging in ArcGIS Pro.

3 Results and discussion

3.1 THg in lichen from background, reservoir and ore-processing areas

Lichens separated by species were collected from six general locations in the surrounding region of the NAMD (Figure 1, locations B1-B6) to assess baseline THg concentrations and variation between species. The results are tabulated in Table 1 and shown in Figure 3. The multi-species mean across all samples from background locations was 156.3 ± 48.2 ng g^{-1}, N = 106. THg concentrations by species showed the following trend: US > RM > FL > EP > RF > RL, with differences in the means being insignificant except for RL vs. RM (179 ± 54 vs. 112 ± 25 ng g^{-1}, respectively) (Table 2). For these species, the difference in the inner structure of the thalli may explain their different accumulations of THg (Zvěřina et al., 2018). Previous observations suggest that epiphytic lichens, when exposed to the same gaseous Hg concentrations, hold different amounts of Hg, which can be explained by the lichens having different gas exchange capabilities with the atmosphere (Vannini et al., 2014). RM lichen commonly have thalli >1 m in length, hanging from a tree branch, whereas the thalli of RF lichen are much more compact, rarely >5 cm, perhaps indicating that the degree of free flowing air is a factor. Lichen age in addition to species could also be important in controlling THg concentrations with longer exposure times presumably resulting in lichens accumulating more THg over time. The older age and larger number of exchange sites of the central part of lichen thalli generally result in higher metal concentrations than the edges of the thalli (Vingiani et al., 2015). However, one study showed no significant effect of thalli diameter on THg in concentrations in lichens from Arizona, in addition to

TABLE 2 Mean and standard deviations of THg concentrations in each species of lichens sampled at background locations B1-B6 in Figure 1.

Lichen species	N (# of lichen samples)	Mean THg (ng g^{-1})	Stdev THg (ng g^{-1})	Median THg (ng g^{-1})	Max THg (ng g^{-1})	Min THg (ng g^{-1})
Usnea sp.	14	179.6	40.2	176.2	257.0	109.8
Ramalina menziesii	16	179.1	53.8	172.8	278.4	96.3
Flavopunctelia sp.	22	169.7	35.1	167.1	257.6	105.2
Evernia prunastri	23	162.0	45.7	149.6	253.1	89.5
Ramalina farinacea	15	128.6	47.0	138.1	207.5	53.0
Ramalina leptocarpha	16	112.4	25.1	120.6	137.4	54.0

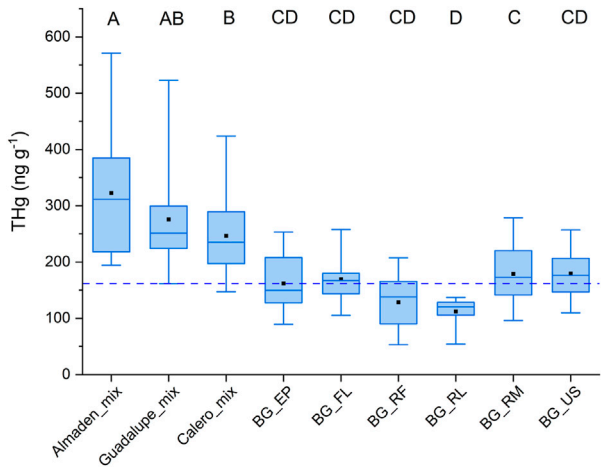

FIGURE 2
Box and whisker plot of Hg concentrations segregated by location and by lichen species. The "BG" locations are the six background sites (Figure 1) from which the data were separated by lichen species. Almaden, Calero, and Guadalupe refer to the sampling locations around each of the reservoirs (R1, R2, and R3 in Figure 1), and "mix" refers to THg concentrations for all lichen species combined. The dashed line represents 156.3 ng g^{-1}, the mean of all the lichen species from the six background locations. The letters above each bar are the groupings from the ANOVA. Categories that do not share a grouping letter have means that are statistically significantly different from one another. The boxes represent the 25th and 75th percentiles, the line in the box is the median, the open square in the box in the mean, and the whiskers are the maximum and minimum.

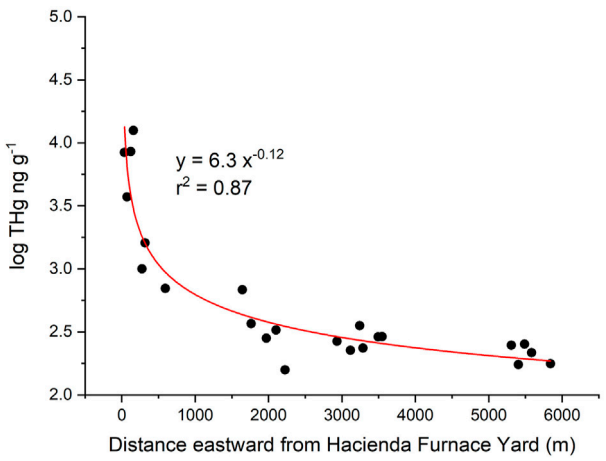

FIGURE 3
THg in lichen collected along a Hacienda Furnace Yard to Calero Reservoir transect. LogTHg plotted is against distance to the east away from the source. The curve intersects the calculated average background THg concentration in lichen (156 ppb) at 7.8 km.

finding no Hg zonation within the thalli (Gremillion et al., 2013). The uptake and accumulation of Hg is complex and likely species specific; however, we sought to minimize these effects by collecting multiple intact clumps of thalli from each location that contained multiple species with thalli of varying ages and homogenizing them into one sample (Barre et al., 2020).

THg concentrations in mixed-species lichens were then determined at locations along the banks of the three reservoirs in the NAMD to assess if Hg deposition was significantly higher than the background all-site mean. Mean THg concentrations were 322.8 ± 123.2, 275.7 ± 90.8, and 246.5 ± 66.2 ng g^{-1} at AR, GR, and CR, respectively, statistically significantly higher than the mean background concentration of 156.3 ± 48.2 ng g^{-1} (Figure 2). The reservoir with the highest THg in lichen (AR), is situated the nearest (1.2 km) to the hotspots at HAC. The Guadalupe Reservoir had the second highest THg in lichen concentrations. Although it is further away from HAC, this location may be influenced by a greater number of smaller mines and former furnace sites in its immediate vicinity (Figure 1). THg concentrations in lichen were lowest at CR and it is located 3.2 km from the HAC site with no historic mining activity in the area between CR and HAC.

To address how far Hg emissions travel from a contaminated hotspot to lichens in cleaner reservoir locations, we sampled along an east-west gradient from HAC to CR (Figure 1). The results are shown in Figure 3 where log-THg concentration is plotted against distance in meters from center of HAC. The data were fit to a power function and used to determine that, at 7.8 km away from HAC, the concentrations of THg in lichen would be at the mean background concentration of 156.3 ng g^{-1}. Note that the distance required to reach background concentrations could vary for different directions based on varying wind patterns. This transect was sampled based on access to public lands and areas owned by the Santa Clara County Parks. Even so, this transect is likely a fair representation of the extent of air pollution from the

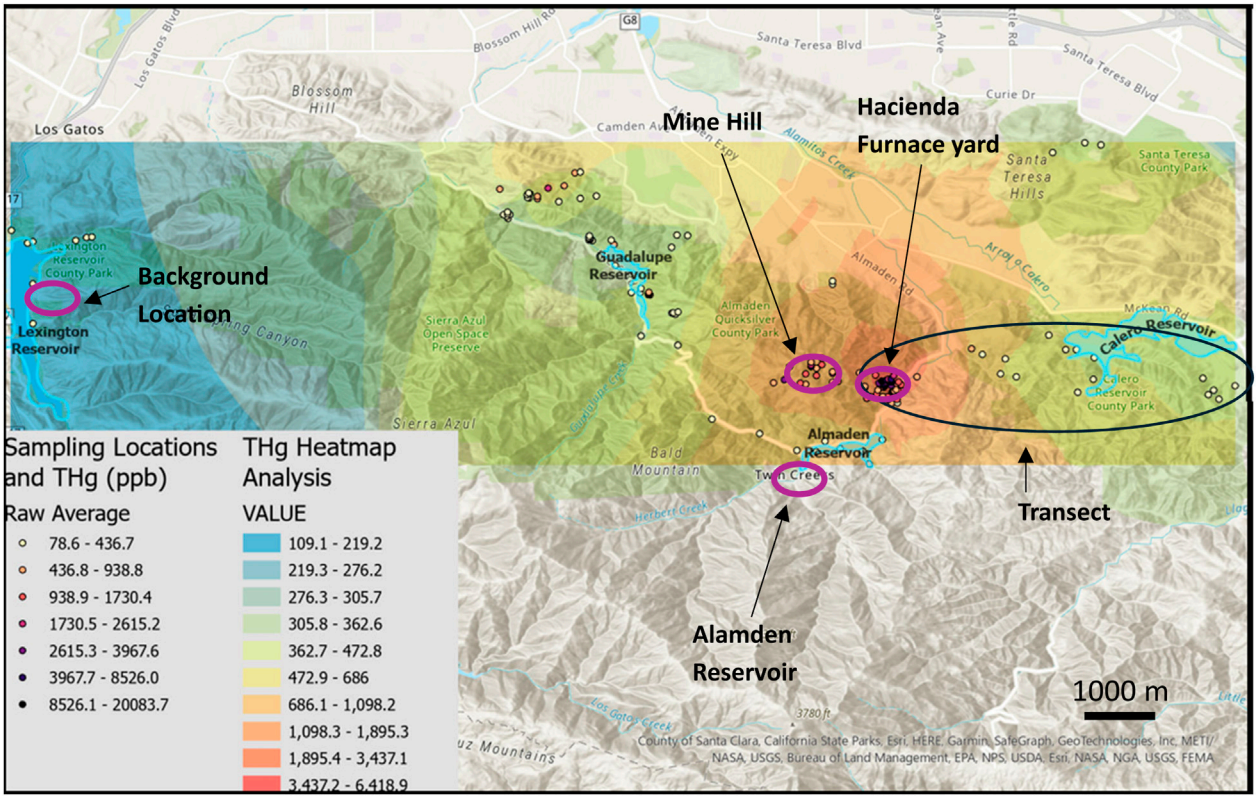

FIGURE 4
Locations of lichen sampling (N = 303) and THg concentrations which were used to generate a heat map analysis for the region. The circled regions in purple are the locations of the transplantation experiment (Figures 5, 6) and the black circle shows the location of the Hacienda–Calero transect in this figure.

mines since it begins at the center of most intense mining and ore processing activities and ends at the far end of CR where no mining activities occurred. Therefore, despite the influences that thalli age and lichen species might have on the *in-situ* THg concentration, we conclude that deposition of legacy Hg is the most relevant factor explaining significant higher THg levels in lichens from reservoir areas.

Lichens were collected at known former mines and ore-processing sites in the NAMD with the goal of constructing a map of emissions hotspots across the mining district. The concentrations are summarized in Table 2 and a heat map of the area is shown in Figure 4. The mean THg concentration for the lichen samples from the NAMD was 1801 ± 3,060 ng g^{-1}, N = 172 (Table 1). High THg concentrations (>5 μg g^{-1}) were found in lichens at HAC and nearby Deep Gulch, and also at Mine Hill, and the Senador Mine. The highest concentration (20.1 μg g^{-1}) was found in Deep Gulch, the site of former dumping of calcines from HAC. These levels of Hg contamination in lichen are similar to those found at Alamadén, Spain (32.4 μg g^{-1}) (Jiménez-Moreno et al., 2016). The heat map of THg concentrations for the NAMD shows high emissions in the areas of HAC, Mine Hill, and the northwestern area near the former Senador Mine. HAC is more contaminated than Mine Hill due to primarily pre-1900 ore-processing activities at HAC with associated contaminated calcine formation, compared to primarily mining and more recent retort activities at the Mine Hill location.

3.2 Lichen transplantation experiments

Significant Hg uptake was observed during lichen transplantation at all three contaminated sites (Figure 5A). The first transplantation experiment (January-September) at three NAMD locations produced uptake rate constants in the following order: HAC (0.0027 $days^{-1}$) > MH (0.0021 $days^{-1}$) > AR (0.0011 $days^{-1}$) (Table 3), matching the order of THg concentration in the *in-situ* lichens at these sites (Table 1). The uptake rates were statistically significant at each of these contaminated sites, while both the background and *in-situ* control transplants showed no significant change in THg concentrations relative to their initial levels (Table 2). In terms of a half-time of uptake (i.e., $t_{1/2} = \frac{\ln 2}{k}$), an uptake rate constant of k = 0.0027 $days^{-1}$ results in $t_{1/2}$ = 257 days, which suggests that close to a year is needed to exchange half of the average total Hg concentration in lichen at HAC.

The second transplantation experiment (August-June) was carried out at the most contaminated site HAC, and the background site LR. An increase in THg concentrations was again observed at HAC, and lichens at the background site did not significantly change their THg concentrations. Interestingly, the uptake rate constant at HAC was noticeably more positive in the first 5 months compared to the last 5 months (Figure 5B). The uptake rate constant for the first 5 months was higher, but similar to that found in transplantation #1 (0.0036 vs. 0.0027 $days^{-1}$, respectively),

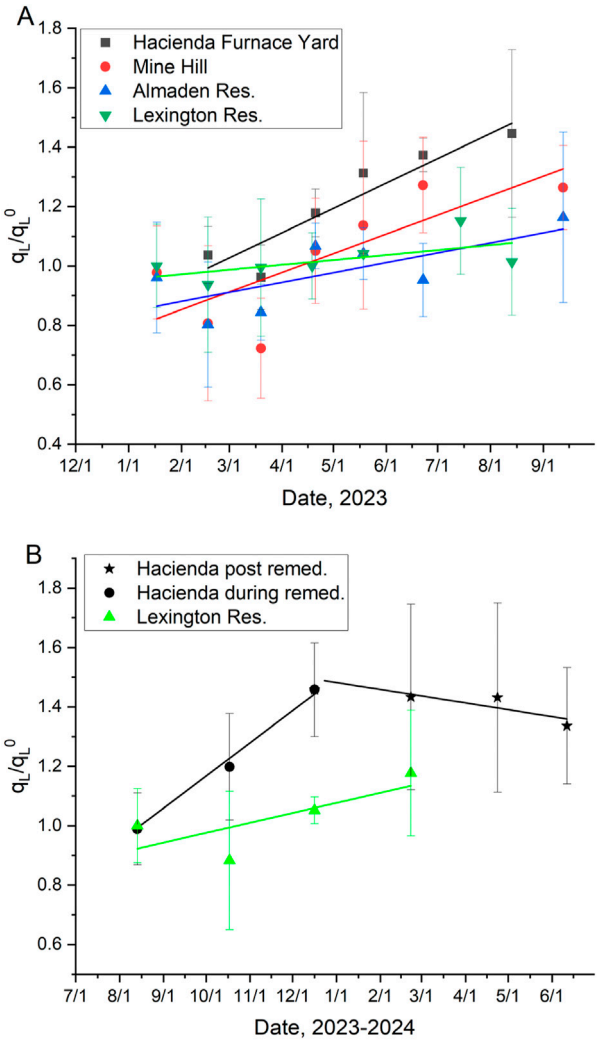

FIGURE 5
Lichen uptake rate constants (q_L/q_L^0) ± 1 s. **(A)** The first transplantation experiment (three locations in the NAMD and the background location), and **(B)** the second transplantation experiment (one location in the NAMD and the background location). The second half of transplantation experiment #2 was separated from the first half showing the potential effects of remediation work at the site, that was completed in early 2024. Linear fit parameters are shown in Table 2.

but for the last 5 months, there was no significant change in THg concentration in the lichen at HAC. We hypothesize that the Deep Gulch Calcines Remediation Project, which ended in March of 2024, could have resulted in lower soil emissions and thus slowed down of the uptake of THg by lichen. If true, this observation underscores the utility of lichen transplantations as methods to detect changing emissions due to clean up efforts at contaminated sites.

The uptake rate constants found here are lower than those found in a previous study at the Almadén mining district in Spain (Berdonces et al., 2017). There, the low end of the slopes from a plot of q_L/q_L^0 vs. time was 0.0033 days^{-1}, which was similar to that found at the NAMD. The largest slopes from that study, however, were five times higher (0.0185 days^{-1}) than what was found in this study, perhaps due to a much larger degree of contamination at that site in Spain.

3.3 Comparison between lichen and passive sampler Hg uptakes rates

This study used Hg passive samplers to compare THg uptake rates with the lichen transplantation experiments. Four MerPAS deployments for 60–65 days spatially matched the lichen transplants during experiment #1, located at AR, MH, HAC, and LR, and during transplantation experiment #2 at HAC and LR. The MerPAS THg uptake rates followed the pattern of HAC > MH > AR > LR (Figure 6), which matched the ranking in contamination between these sites and THg concentrations in the *in-situ* lichen, lending confidence to both the lichen and passive sampler monitoring methods. Comparing only the MerPAS and lichen transplant data at HAC, the MerPAS produced higher uptake rates than the RL lichen in deployments 1 and 3 (27%–37% higher), but in deployment 2, the uptake rate in the RL lichen was 60% higher. Both the RL lichen and the passive samplers showed an increase in uptake during deployments 2 and 3 in the warmer months (Feb-Apr and Aug-Oct) compared with deployment 1 in the colder months (Jan-Mar). This is consistent with higher soil emissions at higher ambient temperatures and more sunlight releasing more Hg^0 to the air (Gustin et al., 2003). Also evident is the difference in uptake rates for different species of lichen in transplant #2 (Aug-Oct) at HAC. The uptake rate by RL lichen was more than double (0.60 ng g^{-1} d^{-1}) that of US lichen, for example, (0.24 ng g^{-1} d^{-1}). Overall, despite the variability in THg concentrations in the lichen, the MerPAS and the lichen transplants produced comparable trends, which confirmed uptake by the lichen due emissions from local contamination.

At the AR and MH sites, in contrast, 60 days was evidently too short to allow for accurate comparison of THg uptake rates from the lichen transplants with the MerPAS. Figure 6 shows negative uptake rates in lichens at these sites. This can also be seen in Figure 5A where the THg concentrations in lichens decreased in the initial part of transplant #1, after which concentrations started to increase. This was observed in the three species transplanted at MH and the two species transplanted at AR. We hypothesize that the loss of Hg initially was due to abnormally cold and wet weather that occurred in Jan-Mar of 2023, which caused the lichen to release Hg not only in these transplants but in the control background transplant at LR as well (Supplementary Figure S4). Regardless of the reason, the negative uptake rates observed reveal the limitations in using lichens to compare with MerPAS in <60 days deployments. Similarly, negative concentration changes in THg concentration in lichen were observed at Spodnja Idrija, Slovenia, 3 km from the Idrija Mines, for the first 6-months after transplantation, after which concentrations increased two-fold after 6-months of exposure (Božič et al., 2022). Here, an uptake rate constant of approximately 0.004 days^{-1} was observed over the whole 12-month period. Thus, for best results, it is advisable to conduct lichen transplantation experiments for a minimum of 12 months if possible.

TABLE 3 Summary of the results of two transplantation experiments.

Type	Exp #	Trans Loc	Lichen origin	N	Time points	Duration (d)	Uptake rate Const (d^{-1})	SE	r^2	p
Uptake	**1**	**AR**	**LR**	**38**	**7**	**238**	**0.0011**	**4E-04**	**0.18**	**0.008**
Uptake	**1**	**MH**	**LR**	**59**	**7**	**238**	**0.0021**	**4E-04**	**0.3**	**8E-06**
Uptake	**1**	**HAC**	**LR**	**45**	**6**	**178**	**0.0027**	**5E-04**	**0.43**	**9E-07**
Uptake	**2**	**HAC**	**LR**	**39**	**4**	**193**	**0.0036**	**5E-04**	**0.64**	**5E-08**
Cont BG	1	LR	LR	19	7	208	0.0005	5E-04	0.1	0.3
Cont *In-Situ*	1	AR	AR	13	7	238	0.0004	5E-04	0.06	0.4
Cont *In-Situ*	1	MH	MH	17	6	156	0.00003	7E-04	1E-04	1
Cont *In-Situ*	1	HAC	HAC	15	5	178	0.0008	0.001	0.03	0.5
Cont BG	2	LR	LR	25	4	193	0.00001	0.001	1E-05	1
Release	1	LR	MH	19	7	208	0.0004	7e-04	0.02	0.6
Release	1	LR	HAC	16	6	178	0.00009	0.001	3e-04	0.9
Release	2	LR	HAC	9	4	193	−0.00001	0.001	1e-05	1

Transplantation types are Uptake, Control Background (Cont BG), Control *In-Situ*, and Release. Transplantation experiment #1 occurred during Jan/Feb–August 2023 and #2 was between August 2023 and June 2024. Locations are abbreviated as AR, MH, HAC, and LR for Almaden Reservoir, Mine Hill, Hacienda Furnace Yard, and Lexington Reservoir, respectively. All the uptake experiments yielded statistically significantly positive uptake rates constants (shown in bold type).

3.4 THg in washed vs. unwashed lichen samples

Selected lichen samples were washed in either DI water (Figure 7A) or 1% EDTA solution (Figure 7B) before homogenization to determine if significant portions of the Hg could be removed from the lichen before analysis. Lichen samples were selected across a range of THg concentrations. There was no difference in the THg results based on washing method and the %RPD between the unwashed and washed groups was 5% ± 30% with unwashed > washed. We found no significant difference in the means of log-transformed THg concentrations between the washed and unwashed groups. For a few of the background samples, the unwashed THg concentration was higher than the washed concentration and could represent Hg-enriched dust particles on the surface of the lichen. However, for the highly contaminated samples taken near the mine sites where there was more exposed soil, no consistent trend was found.

3.5 Hg chemical speciation by HERFD XANES analysis

Three lichen samples from the most contaminated areas in and near the Hacienda Furnace Yard were analyzed using HERFD Hg $L\alpha_1$ XANES spectroscopy to gain insight into molecular Hg speciation. The spectrum of HAC4-1 (bulk THg = 14.8 μg g^{-1}) is dominated by α-HgS(s) (85%) (Figure 8a) and was fit equally well with either a reference natural cinnabar sample or a pure, synthetic compound (Supplementary Table S3). The minor component (~15%) was fit best with a spectrum of natural $Hg_3S_2Cl_2$ (the mineral corderoite) but could also be fit with a combination of other reference spectra with sulfide and chloride ligands. Spectrum HAC4-2 (Figure 8b), collected in a region on the sample with lower Hg counts, was fit with 43% Hg $(cyst)_2$, in which Hg is bonded to two cysteine ligands in a near-linear geometry (Manceau et al., 2015b; Thomas et al., 2019). The remaining fraction of the sample could be fit with a non-unique combination of spectra of natural sulfide reference minerals in the family of tetrahedrite minerals (Cu-Hg-Sb sulfides) and tiemannite (HgSe(s)), which are structurally similar to β-HgS (metacinnabar), and with a fraction α-HgS(s) (~15%, Figure 8c; Supplementary Table S3). The spectrum of AQ30JM4 (bulk THg = 8.39 μg g^{-1}), collected ~1.5 km from HAC at higher elevation, was similar to HAC4-1 and was fit well with the same two components (74% α-HgS(s) and 26%$Hg_3S_2Cl_2$(s)) (Supplementary Figure S5). The spectrum of sample AQ22BM1 (bulk THg = 14.1 μg g^{-1}), collected 200 m from HAC4, was dominated by Hg $(cyst)_2$ (54%), but a secondary component was fit best with a Hg(I) chloride reference spectrum rather than a combination of Hg-sulfide bonding environments (Supplementary Figure S5). There was no evidence in any spectra for Hg^0 as elemental liquid Hg, or for a significant fraction of methylmercury (>10% of the total spectral signal) based on fits with multiple reference spectra.

In the NAMD lichen samples, α-HgS(s), fit using either natural cinnabar spectra or a spectrally identical synthetic compound, was the major Hg species in two spectra and a secondary species in the other two. The spatial increase in Hg concentration in the sample observed with the dominance of this phase suggests that α-HgS(s) was present as particles in the range of nano-to micro-meter size. In spectra not dominated by α-HgS(s), Hg $(cyst)_2$ or reference spectra with similar absorption features, was a major species. Fits with this component likely represent local Hg-dithiol or dithiolate bonding with linear geometry commonly found for Hg associated with

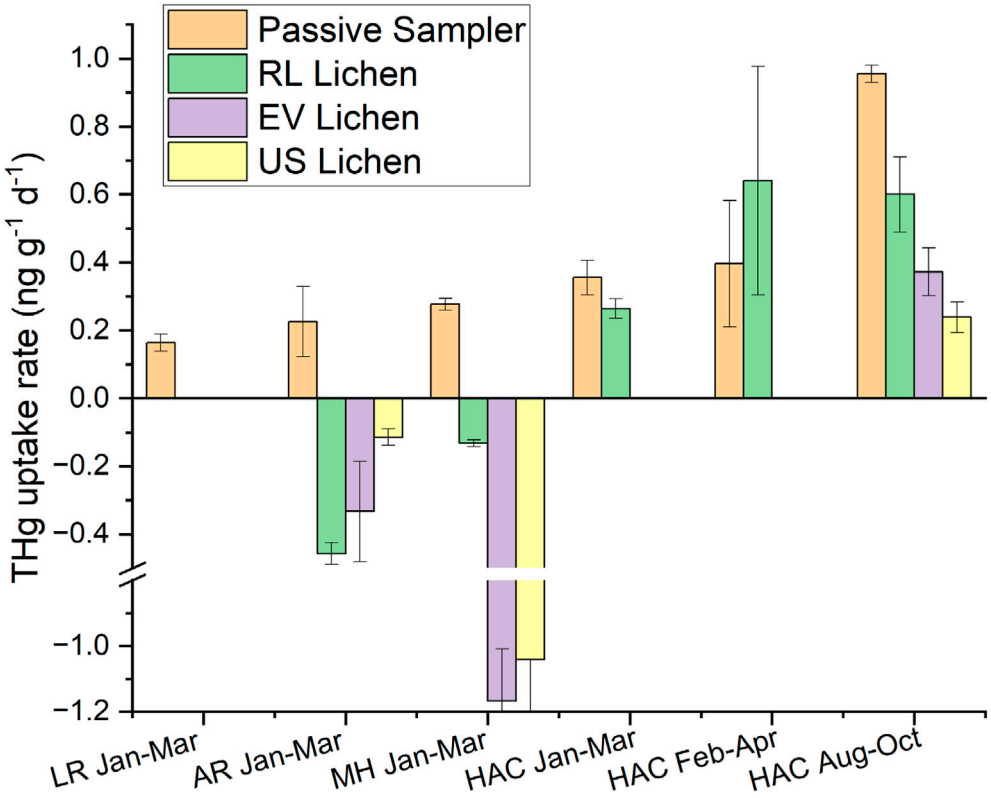

FIGURE 6
THg uptake rates measured with the MerPAS passive samplers and three species of lichens at the four locations during three time periods. LR = Lexington Reservoir (Background site), AR = Almaden Reservoir, MH = Mine Hill, and HAC = Hacienda Furnace Yard. RL = *Ramalina leptocarpha*, EV = *Evernia prunastri*, and US = *Usnea* sp.

reduced sulfur in organic matter and other biological compounds (Manceau et al., 2015a; Thomas et al., 2019; Isaure et al., 2020). Spectral fits with a wide range of reference spectra for secondary components suggest minor Hg bonding to other sulfide and chloride ligands. Interestingly, β-HgS (metacinnabar) was not identified as a component in any spectra, although the secondary components in spectrum HAC4-2 could be fit with a combination of natural mineral spectra (tetrahedrite and tiemannite) that are structurally similar to β-HgS(s). Bulk sample trace element analysis of the lichens showed Se concentrations between 0.2–0.4 μg g^{-1}, concentrations of Cu, Zn, and other transition metals from ~10–70 μg g^{-1}, and Fe concentrations between 1,400–4,800 μg g^{-1} (Supplementary Figure S6). These elements may substitute into a mixed sulfide phase such as Hg-tetrahedrite (nominally $(Cu, Hg, Zn, Fe, Mn)_6(Cu)_6(Sb, As, Se)_4S_{13}$; Foit and Hughes, 2004), and Se concentrations compared to Hg permissively allow for the presence of trace tiemannite (HgSe(s)). The HERFD XANES spectra of the two HgS(s) polymorphs, α-HgS(cinnabar) and β-HgS(metacinnabar), are distinct and readily distinguished in spectral mixtures. Also, β-HgS(s) is known to convert to α-HgS(s), the thermodynamically more stable form, over time at ambient temperature and pressure, although the presence of Fe, Zn, Se, or other substituent elements has been reported to stabilize metacinnabar (Dickson and Tunell, 1959).

As noted above, Hg speciation in lichens have not been studied previously by HERFD XANES. The closest comparisons come from Hg HERFD XANES analysis of plant leaves (Manceau et al., 2018) and bark (Bardelli et al., 2022). These studies reported nanoparticle β-HgS(s), not α-HgS(s), as the major Hg-sulfide species in addition to Hg-dithiol coordination. Although α-HgS(s) was identified as a spectral component in nearby soils in these prior studies, physical assimilation of dust particles by leaves or bark was ruled out as a source of nanoparticle β-HgS(s). Likewise for our study, sample washing prior to homogenization removed surface dust, and lichen age of 2–14 years (Stone and McCune, 1990) indicates that current samples are too young to have been alive during active mining (prior to ~1970). However, we cannot rule out assimilation of wind-blown soil containing particulate α-HgS(s) as lichens are known for their ability to trap particles on outer surfaces of the hyphal network and store them in intracellular spaces of the medullary region (Thakur et al., 2024).

The cellular mechanisms by which atmospheric Hg is acquired by lichens and converted to bound species within the organism are not known in detail. Studies suggest a period of dynamic equilibrium of gaseous Hg^0 between lichens and the atmosphere during initial contact that may depend on environmental conditions or seasonal variation (Bargagli, 2016; Ciani et al., 2023; Božič and Horvat, 2024). Conversion of Hg^0 by lichens into other forms is believed to occur via an enzyme-mediated conversion to Hg^{II} followed by complexation to thiol groups of proteins, possibly associated with phytochelatins as a detoxification mechanism (Bargagli, 2016; Seregin and Kozhevnikova, 2023). Wet deposition of atmospheric

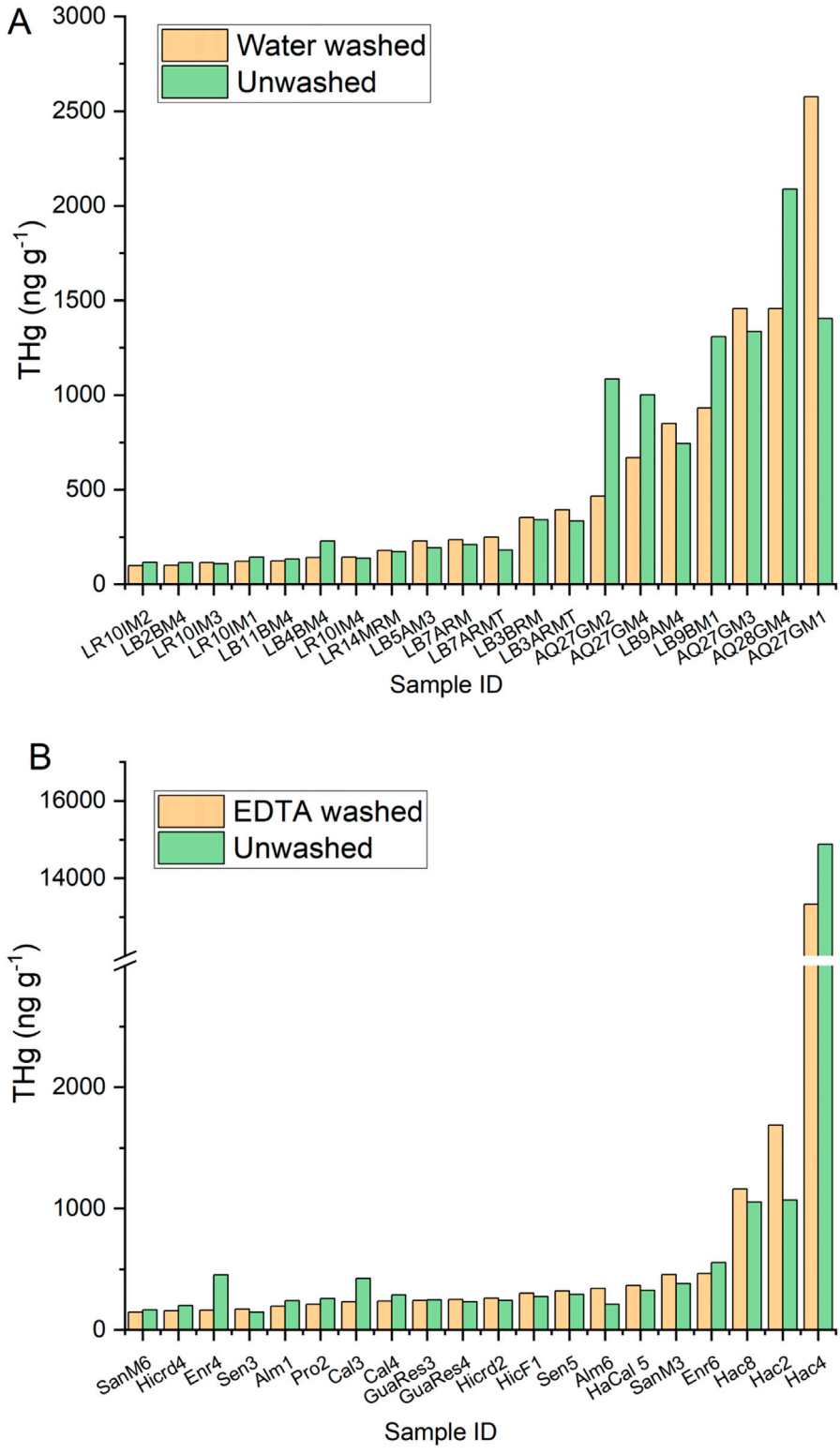

FIGURE 7
THg in mixed species lichen samples across a range of sites from background to contaminated, that were unwashed vs. washed with **(A)** water or **(B)** 1% EDTA prior to analysis.

Hg^{II} species and uptake by lichens and mosses have been documented by Hg isotope evidence, but the oxidized Hg^{II} species are poorly known and likely in dynamic balance with Hg^{0} (Yang et al., 2019; Sonke et al., 2023). Biosynthesis of nanoparticle β-HgS(s) from Hg thiolate or cysteinate compounds has been proposed as a formation pathway in prior Hg HERFD XANES

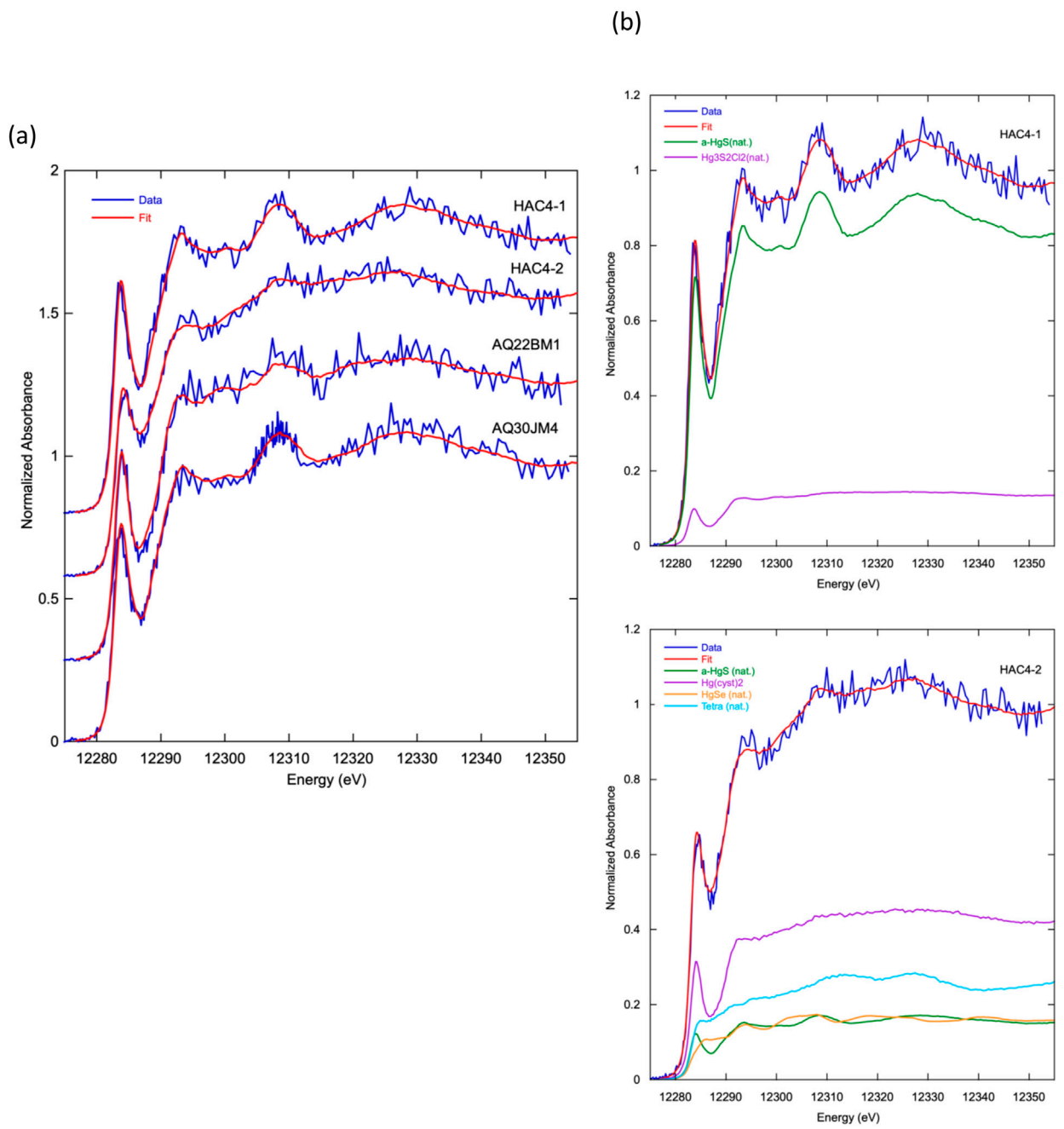

FIGURE 8
Hg Lα1 HERDF XANES spectra and best fits using linear combinations of reference spectra of lichen samples. **(a)** Spectra from three localities in the Hacienda Furnace Yard area of the NAMD; HAC4-1 and HAC4-2 spectra were collected on different regions of the same powered, homogenized sample. **(b)** Fit deconvolutions of HAC4-1 (top) and HAC4-2 (bottom) spectra showing relative contributions of reference spectra: α-HgS(nat.) - natural cinnabar; $Hg_3S_2Cl_2$(nat.) - natural corderoite; Hg $(cyst)_2$ - L-cysteine (aq., 1 mM), pH 2.2; HgSe(nat.) - natural tiemannite; Tetra (nat.). - natural tetrahedrite. Numerical fit results for all four spectra are given in Supplementary Table S3 and fit deconvolutions for the other two samples are shown in Supplementary Figure S5.

studies of plant leaves, bacteria, and bark (Manceau et al., 2018; Thomas et al., 2019; Isaure et al., 2020; Bardelli et al., 2022), but α-HgS(s) was not identified in these biological systems. In their HERFD XANES analysis of Hg speciation in bark near former Hg mines, Bardelli et al. (2022) also found no evidence for Hg^0, and pointed out that Hg bonding with organic compounds is not limited to Hg-dithiol bonds and is likely more complicated, in agreement with our observations of permissive fits to secondary Hg components with compounds representing a variety of Hg ligands and bonding geometries. It is unclear, however, why Hg speciation in the NAMD lichens is dominated by α-HgS(s) rather than β-HgS(s). The samples may be old enough for conversion of β-HgS(s) to α-HgS(s) to occur, nanoparticulate α-HgS(s) may have persisted after entrapment and intracellular storage, or lichens may

possess different pathways than other organisms for biosynthesis of particulate forms of HgS(s) as a means to isolate toxic Hg in their systems. The spectral data showed that Hg in lichens from the HAC area is sequestered mostly in non-volatile phases and species, with no evidence for Hg^0 or methylmercury. Rather, Hg speciation was dominated by α-HgS(s) and to a lesser extent associated with other Hg-sulfide phases and Hg dithiol, sulfide, or chloride ligands.

4 Conclusion

Air emissions of Hg from contaminated soils in the NAMD were mapped out using a convenient and popularly used biomonitor, epiphytic lichens. THg concentrations in lichens sampled in the NAMD were compared against lichens sampled around downstream reservoirs and several reference locations 20–60 km away. This analysis revealed that THg concentrations in lichens were significantly elevated at the three reservoirs in the NAMD by between 93–171 ng g^{-1} over the background, indicating enhanced Hg deposition to the watershed. THg concentrations in lichens sampled along a transect from the most contaminated site HAC to the Calero Reservoir where no mining activity took place showed that background concentrations of lichens was reached at 7.8 km. In addition to HAC, there were areas around Mine Hill and near Guadalupe Reservoir where concentrations of THg in lichens were also elevated (>1 μg g^{-1}).

While collection of *in-situ* lichens allowed for spatial mapping, lichen transplants provided this study with a means of quantifying Hg uptake rates, which represents net Hg deposition to foliage. Two 9-month lichen transplantation experiments were conducted with three lichen species at three locations in the NAMD and one background location. Uptake rate constants were statistically significantly positive at all three sites in the NAMD, with their values scaling with the THg concentrations in the *in-situ* lichens (HAC > MH > AR). There was no significant change in THg concentration during the transplants for the background control or the *in-situ* controls. This demonstrated that lichens can be a useful and inexpensive tool for detecting Hg emissions and comparing emissions between sites of varying contamination levels.

Uptake rates of Hg were quantified during four (60–65 days) passive Hg sampler (MerPAS) deployments during which time lichens were also analyzed in the transplantation experiments. The results showed that one species of lichen (RL) at the most contaminated HAC produced uptake rates that agreed to within 30%–46% of the Hg uptake rates measured with the MerPAS. Both methods showed greater uptake during the warmer months consistent with greater soil emissions. Two other lichen species transplanted at HAC also showed positive Hg uptake rates but at 2.5–4 times lower than the MerPAS. Uptake rates in lichens over the MerPAS deployments at MH and AR were negative because of changes in the lichens due to environmental factors and could not be used for a reliable analysis.

Washing experiments, the transplantation Hg release experiments, and HERFD XANES analysis of lichen samples revealed that Hg compounds are held firmly in the lichen tissue and not easily washed off or released in gaseous form, consistent with previous research. Analysis of HERFD XANES spectra showed that Hg in lichens collected at and near HAC is bonded in non-volatile phases and species, with no evidence for Hg^0 or methylmercury, and with most Hg found in α-HgS (cinnabar) and to a lesser extent associated with Hg dithiol, sulfide, or chloride ligands. These results indicate that Hg in lichens in the NAMD can accumulate, as we observed with some samples reaching up to 20 μg g^{-1}, but that the fraction of Hg exchanged with the atmosphere is small, in agreement with the observed positive and negative uptake rates. Therefore, the majority of the Hg in lichens is likely sequestered in insoluble phases and complexes, limiting its direct impact on watershed Hg and loadings to the reservoirs.

Lastly, this study result revealed some weaknesses when using lichens as bioindicators for Hg pollution in a legacy mining district. To get sufficient spatial coverage, multiple lichen species must be sampled that are composed of lichen thalli of differing ages having taken up varying amounts of Hg, necessitating the sampling of sufficient quantities of lichens for homogenization to minimize these effects. Lichen transplants are a cost-effective way to measure Hg deposition rates, but this work found that there are seasonal effects on lichen uptake and release of Hg, which requires longer duration exposures compared with commercially available passive samplers, to get reliable rates.

Data availability statement

The original contributions presented in the study are included in the article/Supplementary Material, further inquiries can be directed to the corresponding author.

Author contributions

PW-P: Conceptualization, Data curation, Formal Analysis, Funding acquisition, Investigation, Methodology, Project administration, Resources, Supervision, Validation, Visualization, Writing – original draft, Writing – review and editing. BS: Investigation, Methodology, Writing – original draft, Writing – review and editing. MR: Investigation, Methodology, Writing – original draft, Writing – review and editing. BZ: Investigation, Methodology, Writing – original draft, Writing – review and editing. MS: Conceptualization, Investigation, Project administration, Resources, Writing – original draft, Writing – review and editing. ER: Formal Analysis, Investigation, Methodology, Writing – original draft, Writing – review and editing. PO'D: Formal Analysis, Investigation, Methodology, Resources, Writing – original draft, Writing – review and editing.

Funding

The author(s) declare that financial support was received for the research and/or publication of this article. This project was funded by U.S. Department of Energy, Office of Environmental Management Minority Serving Institutions Partnership Program (MSIPP) managed by the Savannah River National Laboratory under BSRA contract No. 0000525173. Use of the Stanford Synchrotron Radiation Lightsource, SLAC National Accelerator

Laboratory, is supported by the U.S. Department of Energy, Office of Science, Office of Basic Energy Sciences under Contract No. DE-AC02-76SF00515.

Acknowledgments

We acknowledge the following people for contributing to the project: Sarah E. Janssen, Michael Tate, Carl Lamborg, Michael Cox, Carrie Austin, Daniel Deeds, Charles Alpers, Roberto Rivera, Tarabryn Grismer, Clara Bang, Elizabeth Pechulis, Nettie Calvin, Kit Vu, Matthew Geller, Molly Hoffman, Vanessa Pham, Emily Zheng, Colby Meeker, Santa Clara County Parks, and James Downing.

Conflict of interest

The authors declare that the research was conducted in the absence of any commercial or financial relationships that could be construed as a potential conflict of interest.

Generative AI statement

The author(s) declare that no Generative AI was used in the creation of this manuscript.

Publisher's note

All claims expressed in this article are solely those of the authors and do not necessarily represent those of their affiliated organizations, or those of the publisher, the editors and the reviewers. Any product that may be evaluated in this article, or claim that may be made by its manufacturer, is not guaranteed or endorsed by the publisher.

Supplementary material

The Supplementary Material for this article can be found online at: https://www.frontiersin.org/articles/10.3389/fenvc.2025.1568188/full#supplementary-material

References

Abas, A. (2021). A systematic review on biomonitoring using lichen as the biological indicator: a decade of practices, progress and challenges. *Ecol. Indic.* 121, 107197. doi:10.1016/j.ecolind.2020.107197

Adamo, P., Bargagli, R., Giordano, S., Modenesi, P., Monaci, F., Pittao, E. L. E. N. A., et al. (2008). Natural and pre-treatments induced variability in the chemical composition and morphology of lichens and mosses selected for active monitoring of airborne elements. *Environ. Pollut.* 152 (1), 11–19. doi:10.1016/j.envpol.2007.06.008

Anderson, J., Lévesque, N., Caron, F., Beckett, P., and Spiers, G. A. (2022). A review on the use of lichens as a biomonitoring tool for environmental radioactivity. *J. Environ. Radioact.* 243, 106797. doi:10.1016/j.jenvrad.2021.106797

Bailey, E. H., and Everhart, D. L. (1964). *Geology and quicksilver deposits of the New Almaden district*, 360. Santa Clara, California: US Government Printing Office.

Bardelli, F., Rimondi, V., Lattanzi, P., Rovezzi, M., Isaure, M. P., Giaccherini, A., et al. (2022). Pinus nigra bark from a mercury mining district studied with high resolution XANES spectroscopy. *Environ. Sci. Process. & Impacts* 24 (10), 1748–1757. doi:10.1039/d2em00239f

Bargagli, R. (2016). Moss and lichen biomonitoring of atmospheric mercury: a review. *Sci. Total Environ.* 572, 216–231. doi:10.1016/j.scitotenv.2016.07.202

Barkay, T., and Gu, B. (2022). Demethylation—The other side of the mercury methylation coin: a critical review. *ACS Environ. Au* 2, 77–97. doi:10.1021/acsenvironau.1c00022

Barre, J. P., Queipo-Abad, S., Sola-Larrañaga, C., Deletraz, G., Bérail, S., Tessier, E., et al. (2020). Comparison of the isotopic composition of Hg and Pb in two atmospheric bioaccumulators in a Pyrenean beech forest (Iraty Forest, Western Pyrenees, France/Spain). *Front. Environ. Chem.* 1, 582001. doi:10.3389/fenvc.2020.582001

Berdonces, M. A. L., Higueras, P. L., Fernández-Pascual, M., Borreguero, A. M., and Carmona, M. (2017). The role of native lichens in the biomonitoring of gaseous mercury at contaminated sites. *J. Environ. Manag.* 186, 207–213. doi:10.1016/j.jenvman.2016.04.047

Božič, D., and Horvat, M. (2024). Insights into seasonal variations in mercury isotope composition of lichens. *Environ. Pollut.* 340, 122740. doi:10.1016/j.envpol.2023.122740

Božič, D., Živković, I., Hudobivnik, M. J., Kotnik, J., Amouroux, D., Štrok, M., et al. (2022). Fractionation of mercury stable isotopes in lichens. *Chemosphere* 309, 136592. doi:10.1016/j.chemosphere.2022.136592

Bubach, D. F., Catán, S. P., Arribére, M. A., Diéguez, M. C., García, P. E., and Messuti, M. I. (2024). Mercury content and elemental composition of fruticose lichens from Nahuel Huapi National park (Patagonia, Argentina): time trends in transplanted and *in situ* grown thalli. *Atmos. Pollut. Res.* 15 (2), 101988. doi:10.1016/j.apr.2023.101988

Capozzi, F., Sorrentino, M. C., Granata, A., Vergara, A., Alberico, M., Rossi, M., et al. (2023). Optimizing moss and lichen transplants as biomonitors of airborne anthropogenic microfibers. *Biology* 12 (10), 1278. doi:10.3390/biology12101278

Cargill, S. M., Root, D. H., and Bailey, E. H. (1980). Resource estimation from historical data: mercury, a test case. *J. Int. Assoc. Math. Geol.* 12, 489–522. doi:10.1007/bf01028882

Carrasco-Gil, S., Siebner, H., Leduc, D. L., Webb, S. M., Millán, R., Andrews, J. C., et al. (2013). Mercury localization and speciation in plants grown hydroponically or in a natural environment. *Environ. Sci. & Technol.* 47, 3082–3090. doi:10.1021/es303310t

Chiarantini, L., Rimondi, V., Bardelli, F., Benvenuti, M., Cosio, C., Costagliola, P., et al. (2017). Mercury speciation in Pinus nigra barks from Monte Amiata (Italy): an X-ray absorption spectroscopy study. *Environ. Pollut.* 227, 83–88. doi:10.1016/j.envpol.2017.04.038

Ciani, F., Fornasaro, S., Benesperi, R., Bianchi, E., Cabassi, J., Di Nuzzo, L., et al. (2023). Mercury accumulation efficiency of different biomonitors in indoor environments: the case study of the Central Italian Herbarium (Florence, Italy). *Environ. Sci. Pollut. Res.* 30 (59), 124232–124244. doi:10.1007/s11356-023-31105-3

Conaway, C. H., Watson, E. B., Flanders, J. R., and Flegal, A. R. (2004). Mercury deposition in a tidal marsh of south San Francisco Bay downstream of the historic New Almaden mining district, California. *Mar. Chem.* 90 (1-4), 175–184. doi:10.1016/j.marchem.2004.02.023

Conti, M. E., and Cecchetti, G. (2001). Biological monitoring: lichens as bioindicators of air pollution assessment—a review. *Environ. Pollut.* 114 (3), 471–492. doi:10.1016/s0269-7491(00)00224-4

Demková, L., Bobuľská, L., Harangozo, Ľ., and Árvay, J. (2023). Using bio-monitors to determine the mercury air pollution in a former mining area. *Eng. Proc.* 57 (1), 28. doi:10.3390/engproc2023057028

Dickson, F. W., and Tunell, G. (1959). The stability relations of cinnabar and metacinnabar. *Am. Mineralogist* 44, 471–487.

Eckley, C. S., Eagles-Smith, C., Luxton, T. P., Hoffman, J., and Janssen, S. (2023). Using mercury stable isotope fractionation to identify the contribution of historical mercury mining sources present in downstream water, sediment and fish. *Front. Environ. Chem.* 4, 1096199. doi:10.3389/fenvc.2023.1096199

Eckley, C. S., Gilmour, C. C., Janssen, S., Luxton, T. P., Randall, P. M., Whalin, L., et al. (2020). The assessment and remediation of mercury contaminated sites: a review of current approaches. *Sci. Total Environ.* 707, 136031. doi:10.1016/j.scitotenv.2019.136031

Fantozzi, L., Ferrara, R., Dini, F., Tamburello, L., Pirrone, N., and Sprovieri, F. (2013). Study on the reduction of atmospheric mercury emissions from mine waste enriched soils through native grass cover in the Mt. Amiata region of Italy. *Environ. Res.* 125, 69–74. doi:10.1016/j.envres.2013.02.004

Foit, F. F., Jr., and Hughes, J. M. (2004). Structural variations in mercurian tetrahedrite. *Am. Mineralogist* 89, 159–163. doi:10.2138/am-2004-0118

Gačnik, J., Živković, I., Kotnik, J., Božič, D., Tassone, A., Naccarato, A., et al. (2024). Comparison of active measurements, lichen biomonitoring, and passive sampling for

atmospheric mercury monitoring. *Environ. Sci. Pollut. Res.* 31 (24), 35800–35810. doi:10.1007/s11356-024-33582-6

Garty, J. (2001). Biomonitoring atmospheric heavy metals with lichens: theory and application. *Crit. Rev. plant Sci.* 20 (4), 309–371. doi:10.1080/20013591099254

Gehrke, G. E., Blum, J. D., and Marvin-DiPasquale, M. (2011). Sources of mercury to San Francisco Bay surface sediment as revealed by mercury stable isotopes. *Geochimica Cosmochimica Acta* 75 (3), 691–705. doi:10.1016/j.gca.2010.11.012

Glatzel, P., Weng, T.-C., Kvashnina, K., Swarbrick, J., Sikora, M., Gallo, E., et al. (2013). Reflections on hard X-ray photon-in/photon-out spectroscopy for electronic structure studies. *J. Electron Spectrosc. Relat. Phenom.* 188, 17–25. doi:10.1016/j.elspec.2012.09.004

Gremillion, P. T., Hermosillo, E., Sweat, K. G., and Cizdziel, J. V. (2013). Variations in mercury concentration within and across lichen Xanthoparmelia spp. individuals: implications for evaluating histories of contaminant loading and sampling design. *Environ. Chem.* 10 (5), 395–402. doi:10.1071/en13053

Gustin, S. M., Coolbaugh, M., Engle, M., Fitzgerald, B., Keislar, R., Lindberg, S., et al. (2003). Atmospheric mercury emissions from mine wastes and surrounding geologically enriched terrains. *Environ. Geol.* 43, 339–351. doi:10.1007/s00254-002-0630-z

Huang, J. H., Berg, B., Chen, C., Thimonier, A., Schmitt, M., Osterwalder, S., et al. (2023). Predominant contributions through lichen and fine litter to litterfall mercury deposition in a subalpine forest. *Environ. Res.* 229, 116005. doi:10.1016/j.envres.2023.116005

Isaure, M. P., Albertelli, M., Kieffer, I., Tucoulou, R., Petrel, M., Gontier, E., et al. (2020). Relationship between Hg speciation and Hg methylation/demethylation processes in the sulfate-reducing bacterium Pseudodesulfovibrio hydrargyri: evidences from HERFD-XANES and nano-XRF. *Front. Microbiol.* 11, 584715. doi:10.3389/fmicb.2020.584715

Jiménez-Moreno, M., Barre, J. P., Perrot, V., Bérail, S., Martín-Doimeadios, R. C. R., and Amouroux, D. (2016). Sources and fate of mercury pollution in Almadén mining district (Spain): evidences from mercury isotopic compositions in sediments and lichens. *Chemosphere* 147, 430–438. doi:10.1016/j.chemosphere.2015.12.094

Jiskra, M., Sonke, J. E., Obrist, D., Bieser, J., Ebinghaus, R., Myhre, C. L., et al. (2018). A vegetation control on seasonal variations in global atmospheric mercury concentrations. *Nat. Geosci.* 11 (4), 244–250. doi:10.1038/s41561-018-0078-8

Kocman, D., Horvat, M., Pirrone, N., and Cinnirella, S. (2013). Contribution of contaminated sites to the global mercury budget. *Environ. Res.* 125, 160–170. doi:10.1016/j.envres.2012.12.011

Ljubič Mlakar, T., Horvat, M., Kotnik, J., Jeran, Z., Vuk, T., Mrak, T., et al. (2011). Biomonitoring with epiphytic lichens as a complementary method for the study of mercury contamination near a cement plant. *Environ. Monit. Assess.* 181, 225–241. doi:10.1007/s10661-010-1825-5

Loppi, S., Pacioni, G., Olivieri, N., and Di Giacomo, F. (1998). Accumulation of trace metals in the lichen Evernia prunastri transplanted at biomonitoring sites in central Italy. *Bryologist* 101, 451–454. doi:10.2307/3244187

Manceau, A., Lemouchi, C., Enescu, M., Gaillot, A. C., Lanson, M., Magnin, V., et al. (2015a). Formation of mercury sulfide from Hg (II)–thiolate complexes in natural organic matter. *Environ. Sci. & Technol.* 49 (16), 9787–9796. doi:10.1021/acs.est.5b02522

Manceau, A., Lemouchi, C., Rovezzi, M., Lanson, M., Glatzel, P., Nagy, K. L., et al. (2015b). Structure, bonding, and stability of mercury complexes with thiolate and thioether ligands from high-resolution XANES spectroscopy and first-principles calculations. *Inorg. Chem.* 54 (24), 11776–11791. doi:10.1021/acs.inorgchem.5b01932

Manceau, A., Wang, J., Rovezzi, M., Glatzel, P., and Feng, X. (2018). Biogenesis of mercury–sulfur nanoparticles in plant leaves from atmospheric gaseous mercury. *Environ. Sci. & Technol.* 52 (7), 3935–3948. doi:10.1021/acs.est.7b05452

McKee, L. J., Bonnema, A., David, N., Davis, J. A., Franz, A., Grace, R., et al. (2017). Long-term variation in concentrations and mass loads in a semi-arid watershed influenced by historic mercury mining and urban pollutant sources. *Sci. Total Environ.* 605, 482–497. doi:10.1016/j.scitotenv.2017.04.203

Monaci, F., Ancora, S., Paoli, L., Loppi, S., and Wania, F. (2022). Lichen transplants as indicators of gaseous elemental mercury concentrations. *Environ. Pollut.* 313, 120189. doi:10.1016/j.envpol.2022.120189

Nash, T. H., III, and Sommerfeld, M. R. (1981). Elemental concentrations in lichens in the area of the four corners power plant, New Mexico. *Environ. Exp. Bot.* 21 (2), 153–162. doi:10.1016/0098-8472(81)90022-8

Nehzati, S., Dolgova, N. V., Young, C. G., James, A. K., Cotelesage, J. J. H., Sokaras, D., et al. (2022). Mercury Lα1 high energy resolution fluorescence detected X-ray absorption spectroscopy: a versatile speciation probe for mercury. *Inorg. Chem.* 61, 5201–5214. doi:10.1021/acs.inorgchem.1c03196

Pirrone, N., Cinnirella, S., Feng, X., Finkelman, R. B., Friedli, H. R., Leaner, J., et al. (2010). Global mercury emissions to the atmosphere from anthropogenic and natural sources. *Atmos. Chem. Phys.* 10 (13), 5951–5964. doi:10.5194/acp-10-5951-2010

Root, H. T., Geiser, L. H., Fenn, M. E., Jovan, S., Hutten, M. A., Ahuja, S., et al. (2013). A simple tool for estimating throughfall nitrogen deposition in forests of western North America using lichens. *For. Ecol. Manag.* 306, 1–8. doi:10.1016/j.foreco.2013.06.028

Rope, S. K., and Pearson, L. C. (1990). *Lichens as air pollution biomonitors in a semiarid environment in Idaho*. Bryologist, 50–61.

Seelos, M., Beutel, M., Austin, C. M., Wilkinson, E., and Leal, C. (2021). Effects of hypolimnetic oxygenation on fish tissue mercury in reservoirs near the new Almaden Mining District, California, USA. *Environ. Pollut.* 268, 115759. doi:10.1016/j.envpol.2020.115759

Selin, N. E. (2009). Global biogeochemical cycling of mercury: a review. *Annu. Rev. Environ. Resour.* 34 (1), 43–63. doi:10.1146/annurev.environ.051308.084314

Seregin, I. V., and Kozhevnikova, A. D. (2023). Phytochelatins: sulfur-containing metal(loid)-chelating ligands in plants. *Int. J. Mol. Sci.* 24 (3), 2430. doi:10.3390/ijms24032430

Sokaras, D., Weng, T. C., Nordlund, D., Alonso-Mori, R., Velikov, P., Wenger, D., et al. (2013). A seven-crystal johann-type hard x-ray spectrometer at the Stanford synchrotron radiation Lightsource. *Rev. Sci. Instrum.* 84 (5), 053102. doi:10.1063/1.4803669

Sonke, J. E., Angot, H., Zhang, Y., Poulain, A., Björn, E., and Schartup, A. (2023). Global change effects on biogeochemical mercury cycling. *Ambio* 52 (5), 853–876. doi:10.1007/s13280-023-01855-y

Sonke, J. E., Shevchenko, V. P., Prunier, J., Sun, R., Prokushkin, A. S., and Pokrovsky, O. S. (2022). Mercury stable isotope composition of lichens and mosses from Northern Eurasia reveals Hg deposition pathways and sources. *ACS Earth Space Chem.* 7 (1), 204–211. doi:10.1021/acsearthspacechem.2c00297

Stone, D. F., and McCune, B. (1990). *Annual branching in the lichen Evernia prunastri in Oregon*. Bryologist, 32–36.

Sun, R., Enrico, M., Heimbürger, L. E., Scott, C., and Sonke, J. E. (2013). A double-stage tube furnace—acid-trapping protocol for the pre-concentration of mercury from solid samples for isotopic analysis. *Anal. Bioanal. Chem.* 405, 6771–6781. doi:10.1007/s00216-013-7152-2

Sweat, K. G. (2010). *Biomonitoring of elemental atmospheric deposition with the lichen Xanthoparmelia spp*. Arizona, USA: Arizona State University.

Thakur, M., Bhardwaj, S., Kumar, V., and Rodrigo-Comino, J. (2024). Lichens as effective bioindicators for monitoring environmental changes: a comprehensive review. *Total Environ. Adv.* 9, 200085. doi:10.1016/j.teadva.2023.200085

Thomas, M. A., Conaway, C. H., Steding, D. J., Marvin-DiPasquale, M., Abu-Saba, K. E., and Flegal, A. R. (2002). Mercury contamination from historic mining in water and sediment, Guadalupe River and San Francisco Bay, California. *Geochem. Explor. Environ. Anal.* 2 (3), 211–217. doi:10.1144/1467-787302-024

Thomas, S. A., Catty, P., Hazemann, J. L., Michaud-Soret, I., and Gaillard, J. F. (2019). The role of cysteine and sulfide in the interplay between microbial Hg (ii) uptake and sulfur metabolism. *Metallomics* 11 (7), 1219–1229. doi:10.1039/c9mt00077a

Vannini, A., Nicolardi, V., Bargagli, R., and Loppi, S. (2014). Estimating atmospheric mercury concentrations with lichens. *Environ. Sci. & Technol.* 48 (15), 8754–8759. doi:10.1021/es500866k

Vingiani, S., De Nicola, F., Purvis, W. O., Concha-Grana, E., Muniategui-Lorenzo, S., López-Mahía, P., et al. (2015). Active biomonitoring of heavy metals and PAHs with mosses and lichens: a case study in the cities of Naples and London. *Water, Air, & Soil Pollut.* 226, 240–312. doi:10.1007/s11270-015-2504-5

Weissman, L., Garty, J., and Hochman, A. (2005). Characterization of enzymatic antioxidants in the lichen Ramalina lacera and their response to rehydration. *Appl. Environ. Microbiol.* 71 (11), 6508–6514. doi:10.1128/aem.71.11.6508-6514.2005

Weiss-Penzias, P. S., Bank, M. S., Clifford, D. L., Torregrosa, A., Zheng, B., Lin, W., et al. (2019). Marine fog inputs appear to increase methylmercury bioaccumulation in a coastal terrestrial food web. *Sci. Rep.* 9 (1), 17611. doi:10.1038/s41598-019-54056-7

Wiederhold, J. G., Smith, R. S., Siebner, H., Jew, A. D., Brown Jr, G. E., Bourdon, B., et al. (2013). Mercury isotope signatures as tracers for Hg cycling at the New Idria Hg mine. *Environ. Sci. & Technol.* 47 (12), 6137–6145. doi:10.1021/es305245z

Will-Wolf, S., Jovan, S., and Amacher, M. C. (2017). Lichen elemental content bioindicators for air quality in upper Midwest, USA: a model for large-scale monitoring. *Ecol. Indic.* 78, 253–263. doi:10.1016/j.ecolind.2017.03.017

Windham-Myers, L., Marvin-DiPasquale, M., Kakouros, E., Agee, J. L., Kieu, L. H., Stricker, C. A., et al. (2014). Mercury cycling in agricultural and managed wetlands of California, USA: seasonal influences of vegetation on mercury methylation, storage, and transport. *Sci. Total Environ.* 484, 308–318. doi:10.1016/j.scitotenv.2013.05.027

Yang, X., Jiskra, M., and Sonke, J. E. (2019). Experimental rainwater divalent mercury speciation and photoreduction rates in the presence of halides and organic carbon. *Sci. Total Environ.* 697, 133821. doi:10.1016/j.scitotenv.2019.133821

Zvěřina, O., Coufalík, P., Barták, M., Petrov, M., and Komárek, J. (2018). The contents and distributions of cadmium, mercury, and lead in Usnea Antarctica lichens from Solorina Valley, James Ross Island (Antarctica). *Environ. Monit. Assess.* 190, 1–9. doi:10.1007/s10661-017-6397-1